Interdiffusion and Atomic Mobilities in fcc Ni-Mo-Ta Alloys

C. P. Wang[1] · X. Yu[1] · S. Y. Qin[1] · Z. B. Wei[1] · J. B. Zhang[1] · Y. X. Huang[1] ·
Y. H. Guo[1] · Y. Lu[1] · X. J. Liu[1,2]

Abstract Ternary fcc Ni-Mo-Ta diffusion couples annealed at 1473 and 1573 K have been studied by using electron probe microanalysis. Based on the measured concentration-distance profiles and Whittle–Green method, the interdiffusion coefficients were calculated to critically assess the atomic mobilities by means of DICTRA software package. Comprehensive comparisons between calculated and experimental diffusion coefficients show that the atomic mobilities obtained in this work could well reproduce the experimental data. Reasonable agreements between model-predicted diffusion properties and the experimental data indicated that present mobility database can be used to study the diffusion behavior, such as diffusion paths and concentration-distance profiles in the ternary fcc Ni-Mo-Ta alloys.

Keywords atomic mobility · DICTRA · diffusion couples · interdiffusion coefficients · Ni-Mo-Ta alloys

1 Introduction

Ni-based superalloys, due to their excellent physical, chemical, and mechanical properties at high temperatures, have found wide applications in a number of industrial fields, such as aircraft, power stations, and marine propulsion.[1,2] They are often used to make complex high-temperature parts for their excellent overall performance, long life, good corrosion and wear resistance at high temperatures. Based on kinetic databases established by the atomic mobility parameters, computational material science methods not only can simulate the evolution of superalloys during processing and service, but also can do further research about various diffusion-related processes, such as solidification, creep, and homogenization.[3] Mo and Ta are two important alloying elements for Ni-based superalloys, as both of them can increase high-temperature strength and enhance the performance of high corrosion resistance.[4,5] However, the introduction of Mo and Ta into Ni-based alloys may have a significant influence upon processing and heat-treatment conditions, as their diffusion characteristics play an indispensable index in microstructure evolution.[3]

CALculation of PHAse Diagram (CALPHAD) has developed rapidly in the past decades so that thermodynamic and kinetic characteristics for multicomponent alloys can be obtained by extrapolation with the aid of related information from lower-order systems.[6] DICTRA is one computational package designed within the CAL-PHAD framework, which can simulate diffusion-controlled processes with the aid of thermodynamic and kinetic databases.[7] Although Ni-based thermodynamic database has been commercialized to aid the design of Ni-based alloys, Ni-based atomic mobility database has been partly reported.[8]

✉ C. P. Wang
wangcp@xmu.edu.cn

Y. Lu
luyong@xmu.edu.cn

X. J. Liu
lxj@xmu.edu.cn

1 College of Materials and Fujian Provincial Key Laboratory of Materials Genome, Xiamen University, Xiamen, People's Republic of China

2 Department of Materials Science and Engineering, Harbin Institute of Technology, Shenzhen, People's Republic of China

The Ni-Mo-Ta ternary system is an important subsystem for Ni-based superalloys, and related studies on its inter-diffusion and atomic mobilities can facilitate the under-standing of related processing design. The atomic mobilities of the fcc Ni-Mo and fcc Ni-Ta binary systems have been reported by Liu et al.[9] and Campbell et al.[8] respectively. However, the atomic mobilities and diffusion characteristic for fcc Ni-Mo-Ta alloys are still lacking. Therefore, in order to establish a general Ni-based super-alloy database, it is essential to assess the atomic mobilities and interdiffusion coefficients of fcc Ni-Mo-Ta alloys within the CALPHAD framework.

The main purposes of the present work are listed as follows: (i) to experimentally measure the interdiffusion coefficients of the fcc Ni-Mo-Ta alloys at the temperature of 1473 and 1573 K with diffusion couples; (ii) to assess the atomic mobilities of the fcc phase for Ni-Mo-Ta alloy system; (iii) to simulate the diffusion paths and concentration profiles with the obtained mobility parameters; (iv) to examine the consistency between the simulated results and the experimental data.

2 Evaluation and Modeling of Ternary Diffusivities

2.1 Evaluation of Ternary Diffusion Coefficients

According to Matano–Kirkaldy's method,[10] the diffusion for a component i of concentration C_i in a ternary system can be described by Fick's second law as

Table 1 Summary of the diffusion couples and experimental conditions

No.	Nominal composition, at.%	Temperature, K	Annealing times, s
A1	Ni/Ni-4Mo-6Ta	1473	259,200
A2	Ni/Ni-8Mo-5Ta		
A3	Ni/Ni-13Mo-3Ta		
A4	Ni-4Ta/Ni-4Mo		
A5	Ni-4Ta/Ni-10Mo		
A6	Ni-6Ta/Ni-10Mo		
B1	Ni/Ni-4Mo-6Ta	1573	172,800
B2	Ni/Ni-8Mo-5Ta		
B3	Ni/Ni-13Mo-3Ta		
B4	Ni-6Ta/Ni-4Mo		
B5	Ni-4Ta/Ni-20Mo		

Table 2 Experimental interdiffusion coefficients and DICTRA-extracted diffusivities in fcc Ni-Mo-Ta alloys

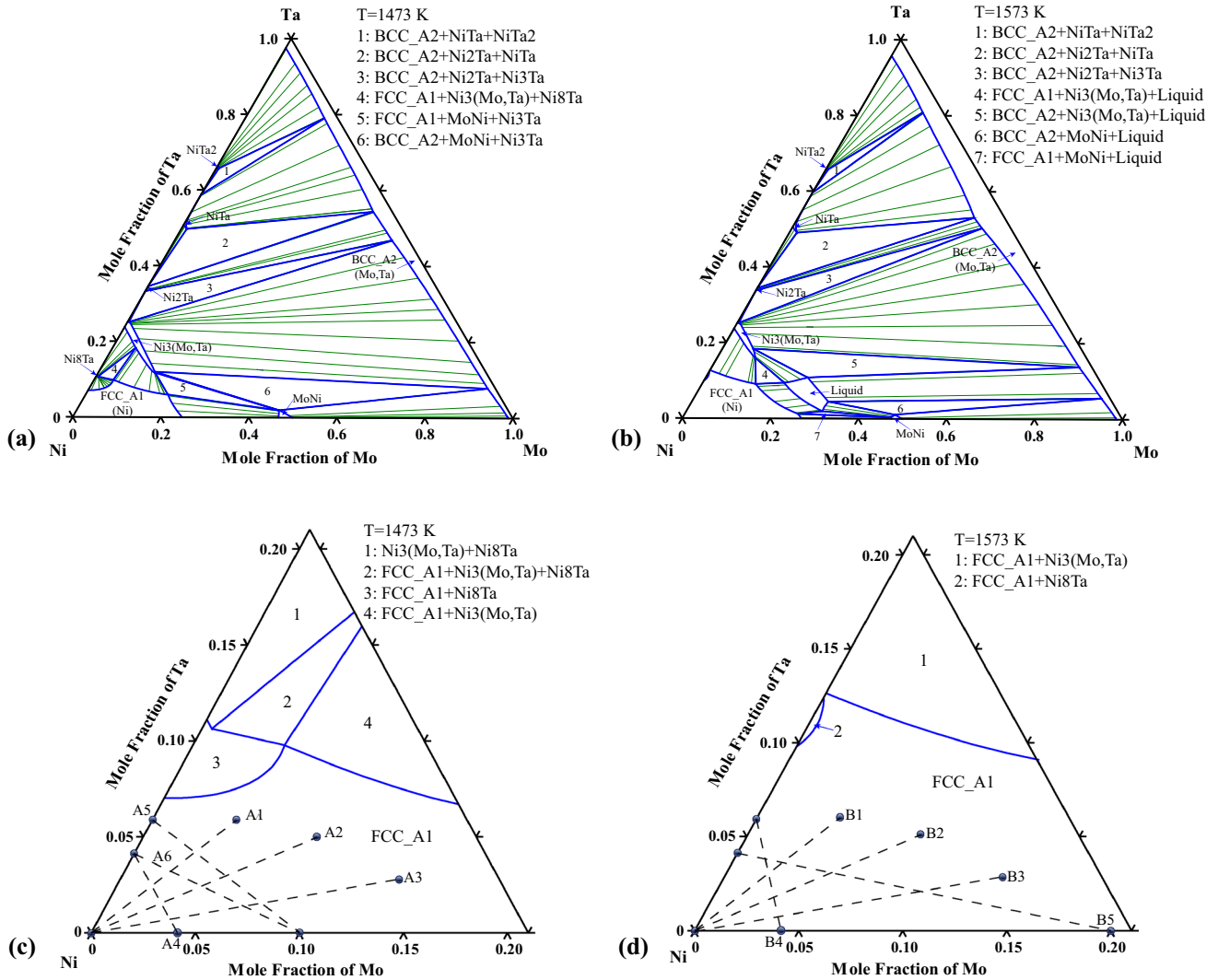| Intersection diffusion paths	Temperature, K	Composition, at.%		Interdiffusion coefficients, 10^{-15} m^2 s^{-1}				DICTRA-extracted diffusivities, 10^{-15} m^2 s^{-1}			
		Mo	Ta	$\tilde{D}^{Ni}_{MoMo}$	$\tilde{D}^{Ni}_{MoTi}$	$\tilde{D}^{Ni}_{TiTi}$	$\tilde{D}^{Ni}_{TiMo}$	$\tilde{D}^{Ni}_{MoMo}$	$\tilde{D}^{Ni}_{MoTi}$	$\tilde{D}^{Ni}_{TiTi}$	$\tilde{D}^{Ni}_{TiMo}$
A1-A4	1473	1.6	2.5	11 ± 10	2 ± 2	26 ± 15	3 ± 3	8	− 0.2	13	− 0.2
A1-A5	1473	2.3	3.3	10 ± 10	2 ± 2	19 ± 10	7 ± 6	7	− 0.2	12	− 0.2
A1-A6	1473	2.9	4.1	9 ± 3	2 ± 2	17 ± 8	6 ± 6	7	− 0.3	10	− 0.3
A2-A4	1473	2.3	1.7	12 ± 4	2 ± 2	26 ± 11	1 ± 1	9	− 0.4	16	− 0.1
A2-A5	1473	4.1	2.4	11 ± 5	3 ± 3	16 ± 5	3 ± 3	6	− 0.3	10	− 0.3
A2-A6	1473	5.1	2.9	10 ± 4	4 ± 4	15 ± 4	3 ± 3	7	− 0.6	13	− 0.2
A3-A4	1473	3.4	1.0	13 ± 5	1 ± 1	35 ± 15	− 0.8 ± 0.9	9	− 0.5	18	0
A3-A5	1473	6.4	1.4	17 ± 10	9 ± 9	18 ± 4	2 ± 2	8	− 1	17	− 0.1
A3-A6	1473	7.3	1.6	11 ± 5	7 ± 8	13 ± 3	2 ± 2	7	− 1	16	− 0.1
B1-B4	1573	2.0	2.9	40 ± 4	6 ± 7	82 ± 30	24 ± 26	44	− 1	52	− 1
B1-B5	1573	2.8	3.9	30 ± 10	12 ± 10	82 ± 40	21 ± 21	41	− 1	44	− 2
B2-B4	1573	2.9	1.8	34 ± 11	1 ± 3	67 ± 20	− 2 ± 2	44	− 2	64	− 0.1
B2-B5	1573	5.4	3.0	29 ± 10	7 ± 8	39 ± 18	10 ± 10	39	− 3	53	− 1
B3-B4	1573	3.4	1.0	39 ± 10	7 ± 8	73 ± 5	− 3 ± 3	46	− 2	74	− 0.3
B3-B5	1573	8.9	1.9	34 ± 5	30 ± 40	40 ± 19	7 ± 7	35	− 6	66	− 0.7

Fig. 1 (a) Calculated isothermal section at 1473 K in Ni-Mo-Ta ternary system using the thermodynamic parameters of Cui et al.,[21] (b) calculated isothermal section at 1573 K in Ni-Mo-Ta ternary system using the thermodynamic parameters of Cui et al.,[21] (c) the diffusion couples in the Ni-Rich area at 1473 K, (d) the diffusion couples in the Ni-Rich area at 1573 K

$$\frac{\partial C_i}{\partial t} = \sum_{j=1}^{2} \frac{\partial}{\partial x}\left(\tilde{D}_{ij}^3 \frac{\partial C_j}{\partial x}\right) \quad \text{for } i = 1, 2 \quad \text{(Eq 1)}$$

where C_i is the concentration of element i, t is the diffusion time, and x is the diffusion distance, $\tilde{D}_{ij}^3$ is the interdiffusion coefficient of the ternary system. When i and j take the same value, the diffusion coefficients, $\tilde{D}_{11}^3$ and $\tilde{D}_{22}^3$, are referred to as the main interdiffusion coefficients. The main diffusion coefficients represent the influence of the concentration gradients of elements 1 and 2 on their own fluxes. When i and j take different values, $\tilde{D}_{12}^3$ and $\tilde{D}_{21}^3$ are called cross interdiffusion coefficients. The cross diffusion coefficients represent the influences of the concentration gradients of element 2 and element 1 on the fluxes of each

other. Under the usual initial and boundary conditions prevalent for semi-infinite diffusion couples, we have

$$C_i(-x, 0) = C_i(-\infty, t) = C_i^-$$
$$C_i(x, 0) = C_i(+\infty, t) = C_i^+ \quad \text{for } i = 1, 2 \quad \text{(Eq 2)}$$

Then the solutions of Eq 1 are:

$$\int_{C_i^-}^{C_i} x\, dC_i = -2t \sum_{j=1}^{2} \tilde{D}_{ij}^3 \frac{dC_j}{dx} \quad \text{(Eq 3)}$$

To avoid the calculating of Matano interface, Whittle and Green[11] introduce the normalized concentration parameter, then the Eq 3 can be transformed to:

Table 3 Assessed mobility parameters for the fcc Ni-Mo-Ta alloys

Atomic mobilities	Parameters, J/mol	References
Mobility of Ni	$\Phi_{Ni}^{Ni} = -276860 + R * T * \text{Ln}\,(8.5E-5)$	22
	$\Phi_{Ni}^{Mo} = -315205 + R * T * \text{Ln}\,(1.27E-4)$	9
	$\Phi_{Ni}^{Ta} = -443736 - 96 * T$	8
	$\Phi_{Ni}^{Ni,Mo} = -153375 - 125 * T$	9
	$\Phi_{Ni}^{Ni,Ta} = -668454$	8
	$\Phi_{Ni}^{Mo,Ta} = -1908437 + 1304 * T$	This work
Mobility of Mo	$\Phi_{Mo}^{Mo} = -254975 + R * T * \text{Ln}\,(5.53E-5)$	9
	$\Phi_{Mo}^{Ni} = -281754.61 + R * T * \text{Ln}\,(1.19E-4)$	9
	$\Phi_{Mo}^{Ta} = -443736 - 96 * T$	This work
	$\Phi_{Mo}^{Mo,Ni} = -60000$	9
	$\Phi_{Mo}^{Ni,Ta} = 2530319 - 1687 * T$	This work
Mobility of Ta	$\Phi_{Ta}^{Ta} = -268253 - 108.6 * T$	8
	$\Phi_{Ta}^{Ni} = -267724 - 79.9 * T$	8
	$\Phi_{Ta}^{Mo} = -315205.34 + R * T * \text{Ln}\,(1.27E-4)$	This work
	$\Phi_{Ta}^{Ta,Ni} = -163380 - 15.97 * T$	8
	$\Phi_{Ta}^{Ni,Mo} = 1185494 - 776.1 * T$	This work
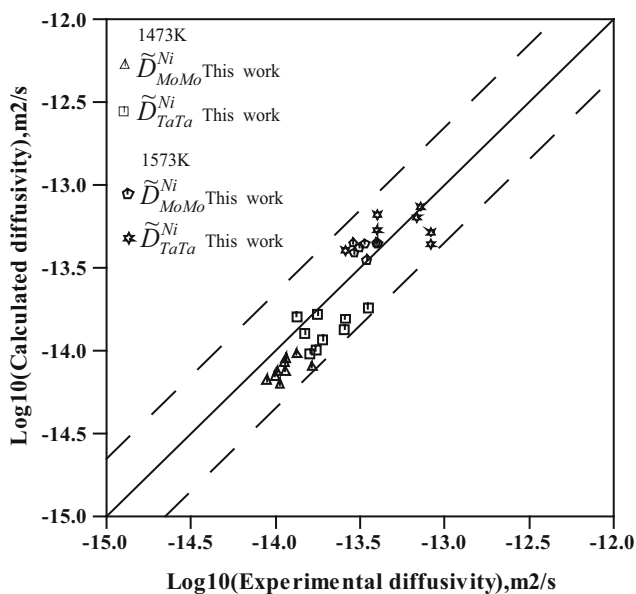
Fig. 2 Comparison between the calculated main interdiffusion coefficients of the fcc Ni-Mo-Ta system and the experimental values at 1473 and 1573 K. Dashed lines refer to the diffusion coefficients with a factor of 2 or 0.5 from the model-predicted ones

$$\frac{1}{2t}\frac{dx}{dY_1}\left[(1-Y_1)\int_{-\infty}^{x} Y_1 \cdot dx + Y_1\int_{x}^{+\infty}(1-Y_1)\cdot dx\right]$$
$$= \tilde{D}_{11}^3 + \tilde{D}_{12}^3\frac{C_2^+ - C_2^-}{C_1^+ - C_1^-}\cdot\frac{dY_2}{dY_1}$$

(Eq 4)

$$\frac{1}{2t}\frac{dx}{dY_2}\left[(1-Y_2)\int_{-\infty}^{x} Y_2 \cdot dx + Y_2\int_{x}^{+\infty}(1-Y_2)\cdot dx\right]$$
$$= \tilde{D}_{22}^3 + \tilde{D}_{21}^3\frac{C_1^+ - C_1^-}{C_2^+ - C_2^-}\cdot\frac{dY_1}{dY_2}$$

(Eq 5)

In order to solve for the four diffusion coefficients in Eq 4 and 5, two diffusion couples whose diffusion paths cross at a common concentration are required.

2.2 Modeling of Atomic Mobility

Based on the absolute reaction rate theory in Ref 12, 13 Anderson and Ågren[14] proposed a method which was similar to the thermodynamic calculation. The atomic mobility M of a component, which is an optimized variable as a function of pressure, temperature and composition. The atomic mobility of element F, M_F, may be divided into a frequency factor M_B^0 and an activation enthalpy Q_B,[14,15] M_B can be described as

$$M_B = M_B^0 \exp\left(-\frac{Q_B}{RT}\right)\frac{1}{RT}{}^{mg}\Gamma$$

(Eq 6)

where R is the gas constant and T is the absolute temperature, ${}^{mg}\Gamma$ is a factor taking into account the effect of the ferromagnetic transition,[16] which is a function of the alloy composition. It has been suggested that one should expand the logarithm of the frequency factor, $\ln M_B^0$ rather than the value itself, thus the mobility, M_B is expressed as
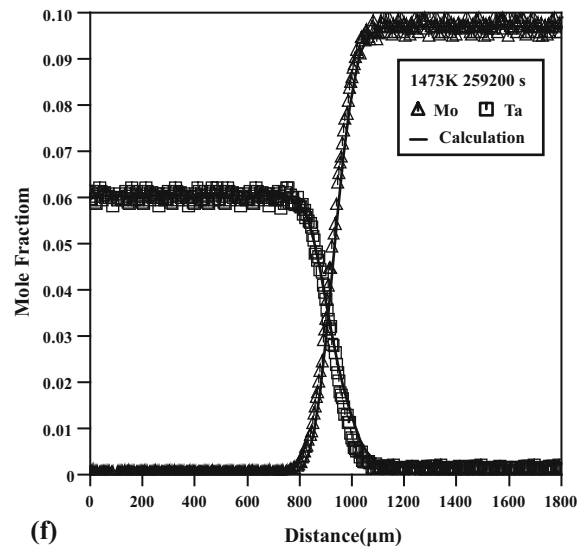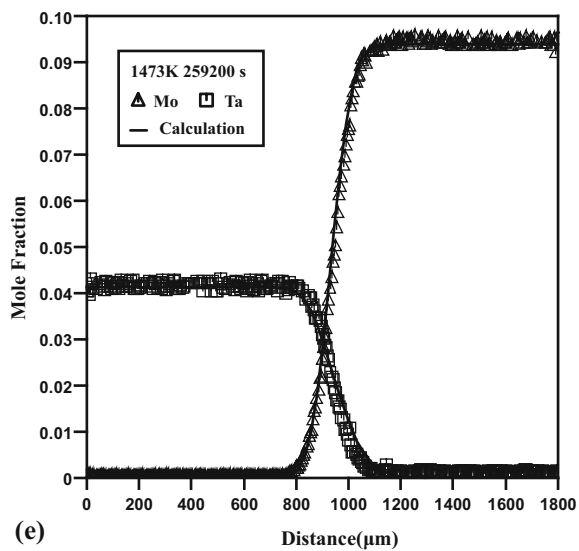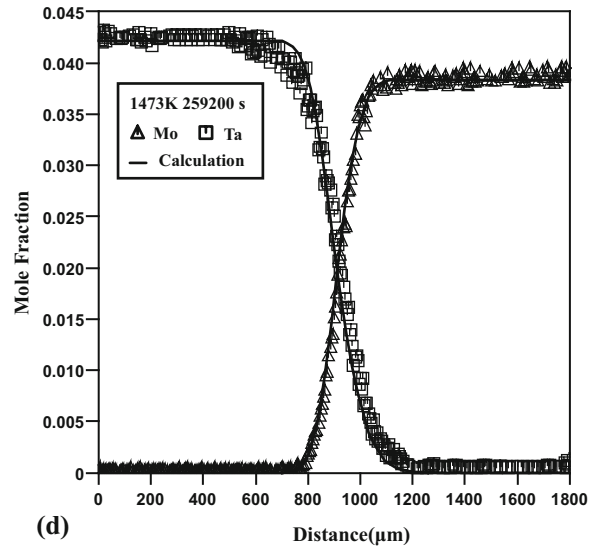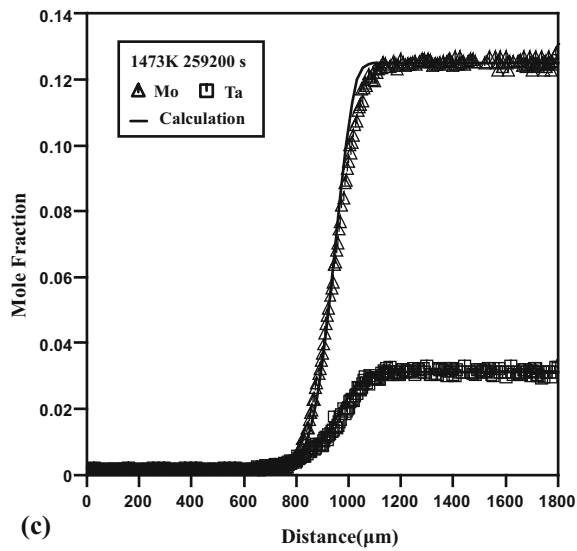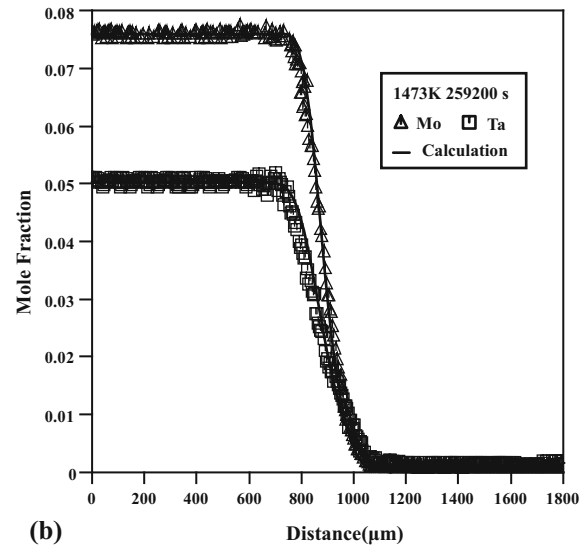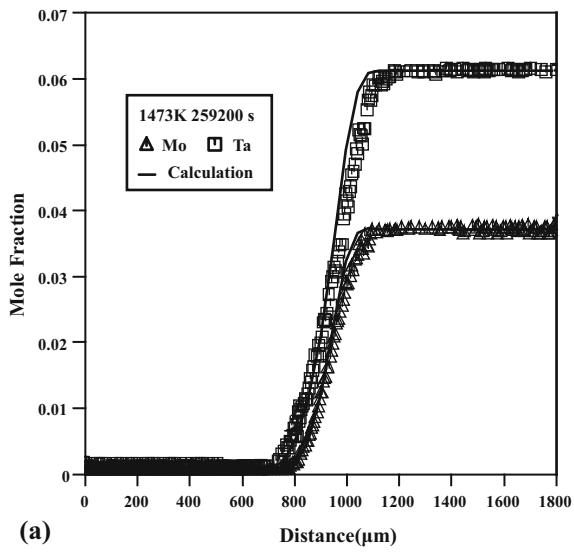
Fig. 3 Comparison between the experimental and DICTRA-simulated concentration profiles for the diffusion couples (a) Ni/Ni-4 at.% Mo-6 at.% Ta, (b) Ni/Ni-8 at.% Mo-5 at.% Ta, (c) Ni/Ni-13 at.% Mo-3 at.% Ta, (d) Ni-4 at.% Ta/Ni-4 at.% Mo, (e) Ni-4 at.% Ta/Ni-10 at.% Mo, (f) Ni-6 at.% Ta/Ni-10 at.% Mo diffusion couples annealed at 1473 K for 259,200 s

$$M_B = \exp\left(\frac{\mathrm{RT} \ln M_B^0}{\mathrm{RT}}\right) \exp\left(-\frac{Q_B}{\mathrm{RT}}\right) \frac{1}{\mathrm{RT}}^{mg} \Gamma \qquad \text{(Eq 7)}$$

For the fcc phase, the ferromagnetic contribution to diffusion is negligible, then M_B^0 and Q_B can be merged into one parameter: $\Phi_B = \mathrm{RT} \ln M_B^0 - Q_B$, Φ_B can be represented by the Redlich–Kister polynomial[17] for binary terms and a power series expansion for ternary terms:[18]

$$\Phi_B = \sum_i x_i \Phi_B^i + \sum_i \sum_{j>i} x_i x_j \left[\sum_{r=0}^m {}^r\Phi_B^{i,j}(x_i - x_j)^r\right] + \sum_i \sum_{j>i} \sum_{k>j} x_i x_j x_k \left[v_{ijk}^s {}^s\Phi_B^{i,j,k}\right] \quad (s = i, j \text{ or } k) \qquad \text{(Eq 8)}$$

where x_i is mole fraction of element i, Φ_B^i is the value of Φ_B for pure i and thus represents one of the endpoint value in the composition space, ${}^r\Phi_B^{i,j}$ and ${}^s\Phi_B^{i,j,k}$ represent binary and ternary interaction parameters. For the parameter v_{ijk}^s, it can be expressed as:

$$v_{ijk}^s = x_s + (1 - x_i - x_j - x_k)/3 \qquad \text{(Eq 9)}$$

where x_i, x_j, x_k and x_s are the mole fractions of elements i, j, k and s, respectively.

The diffusion mobility can be related to the diffusion coefficient, assuming a mono-vacancy mechanism coupled neglecting correlation factors, the tracer diffusivity D_B^* is directly related to the mobility M_B by means of the Einstein relation:

$$D_B^* = \mathrm{RT} M_B \qquad \text{(Eq 10)}$$

The interdiffusion coefficients parameters are related to thermodynamic factors and atomic mobility[19]

$$\tilde{D}_{kj}^n = \sum_i (\delta_{ik} - x_k) \cdot x_i \cdot M_i \cdot \left(\frac{\partial \mu_i}{\partial x_j} - \frac{\partial \mu_i}{\partial x_n}\right) \qquad \text{(Eq 11)}$$

where the Kronecker delta $\delta_{ik} = 1$ when $i = k$, otherwise $\delta_{ik} = 0$. The x_i, μ_i and M_i are the mole fraction, chemical potential and mobility of element i, respectively.

3 Experimental Procedure

Ni (purity: 99.9 wt.%), Mo (purity: 99.9 wt.%) and Ta (purity: 99.9 wt.%) were used as starting materials. Eleven diffusion couples at different temperature, 1473 and

1573 K respectively, were shown in Table 1, which were prepared in the following steps.

First, the samples were melted into alloy ingots by arc melting filled with argon atmosphere to ensure that the composition of each alloy ingot was uniform and homogeneous.

Then, the alloy blocks were linearly cut into blocks in size of $4 \times 4 \times 7$ mm^3 by wire-electrode discharging machining. Following, all the samples were polished on the SiC paper to remove surface contamination. Afterwards, these small bars were vacuum-packed in quartz tubes which were placed in a pit furnace at a temperature of 1473 K to promote homogenization and grain growth. Then, every surface were polished through 0.05 μm alumina for good bonds in the following.

Subsequently, the diffusion couples were fixed by Mo-wires. These diffusion couples were sealed into evacuated quartz tubes and annealed at 1473 K for 259,200 s and 1573 K for 172,800 s, respectively, followed by ice water quenching. And then, the couples were cut along the diffusion direction to expose diffusion interfaces which were polished as before. After standard metallographic preparation, the samples were tested by EPMA (JXA-8100, JEOL, Japan, the accelerating voltage and probe current were 20 kV and 1.0×10^{-8} A, respectively) to measure the local concentration-distance profiles.

4 Results and Discussion

4.1 Measurement of Interdiffusion Coefficients

In this work, four interdiffusion coefficients $\tilde{D}_{MoMo}^{Ni}$, $\tilde{D}_{MoTa}^{Ni}$, $\tilde{D}_{TaTa}^{Ni}$, $\tilde{D}_{TaMo}^{Ni}$ were determined at the intersection composition of the diffusion paths based on the Whittle–Green method, using Eq 4 and 5. Among them, $\tilde{D}_{MoMo}^{Ni}$ and $\tilde{D}_{TaTa}^{Ni}$ are the main interdiffusion coefficients, $\tilde{D}_{MoTa}^{Ni}$ and $\tilde{D}_{TaMo}^{Ni}$ are the corresponding cross coefficients. The experimentally measured main interdiffusion coefficients and the corresponding cross interdiffusion coefficients along with the DICTRA-extracted coefficients are given in Table 2. Multiple sets of interdiffusion coefficients and the standard deviation of these data can be obtained by EPMA. According to these sets of deviations, the maximum acceptable error of the four interdiffusion coefficients can be obtained, which are $\pm 5 \times 10^{-14}$, $\pm 5 \times 10^{-14}$, $\pm 8 \times 10^{-14}$, $\pm 5 \times 10^{-14}$ m^2 s^{-1}. It is observed that the main interdiffusion coefficients are positive, while the cross interdiffusion coefficients are positive and negative, and the value of $\tilde{D}_{TaTa}^{Ni}$ are generally larger than those of $\tilde{D}_{MoMo}^{Ni}$, which indicate that the diffusion rate of Ta is
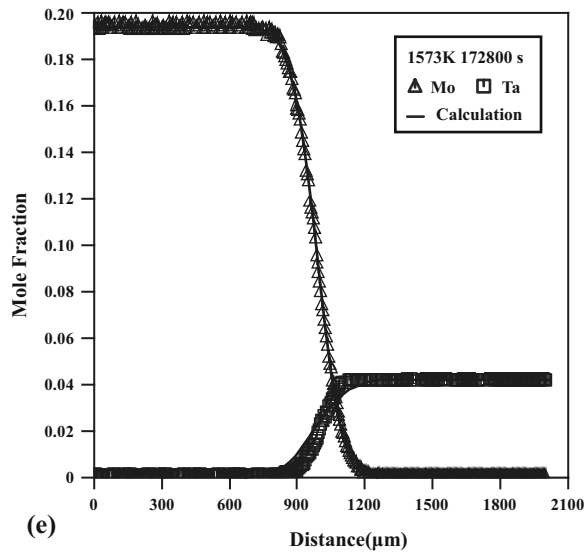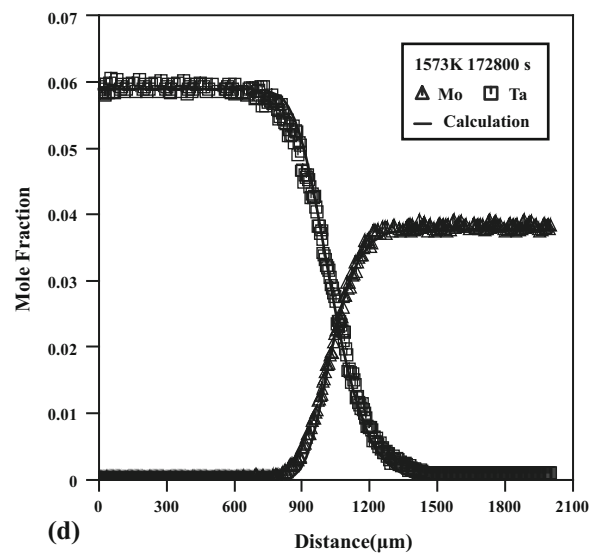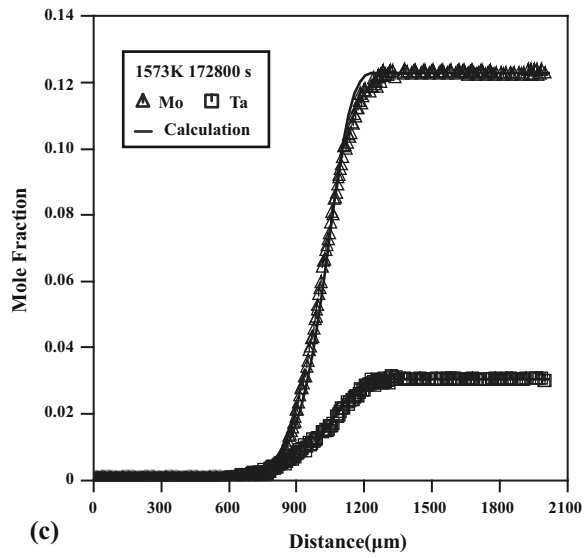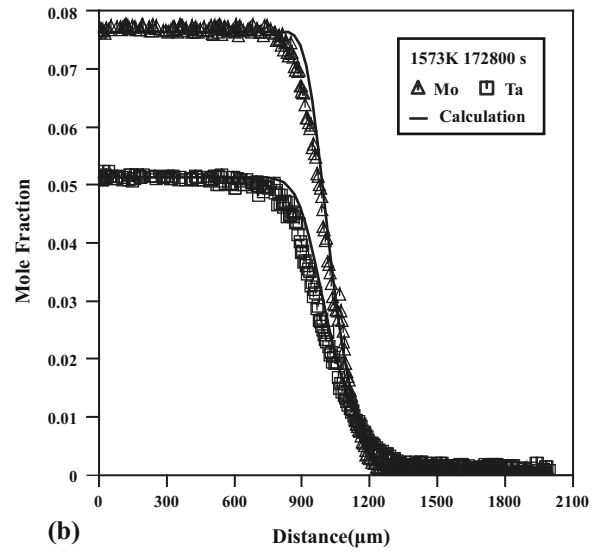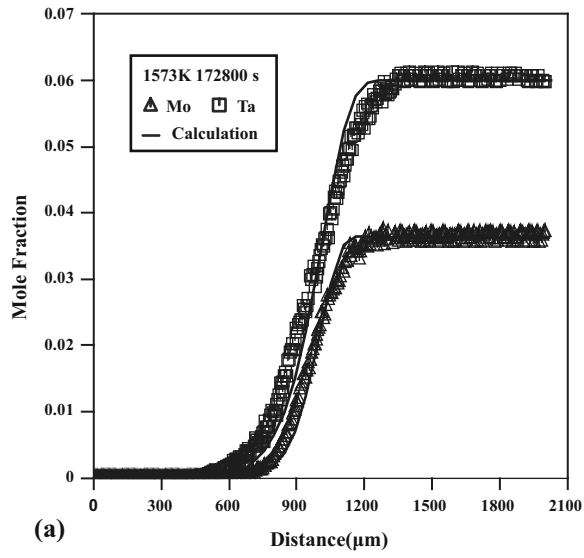
(a)

(b)

(c)

(d)

(e)

◀**Fig. 4** Comparison between the experimental and DICTRA-simulated concentration profiles for the diffusion couples (a) Ni/Ni-4 at.% Mo-6 at.% Ta, (b) Ni/Ni-8 at.% Mo-5 at.% Ta, (c) Ni/Ni-13 at.% Mo-3 at.% Ta, (d) Ni-6 at.% Ta/Ni-4 at.% Mo, (e) Ni-4 at.% Ta/Ni-20 at.% Mo diffusion couples annealed at 1573 K for 172,800 s
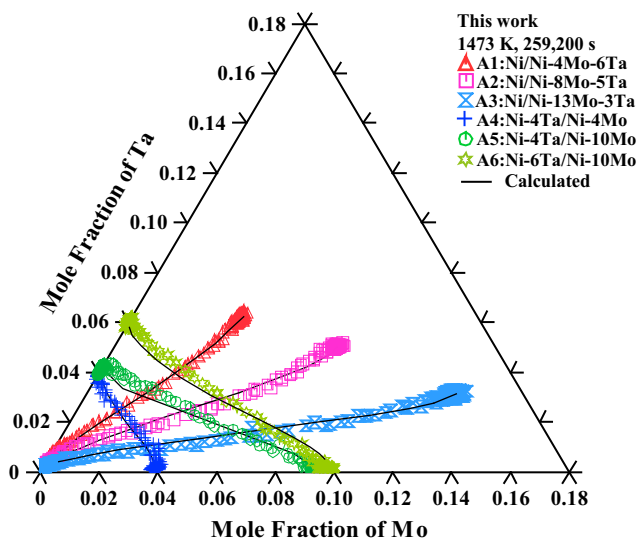

Fig. 5 Comparison between the experimental and DICTRA-simulated diffusion paths for various ternary Ni-Mo-Ta diffusion couples annealed at 1473 for 259,200 s
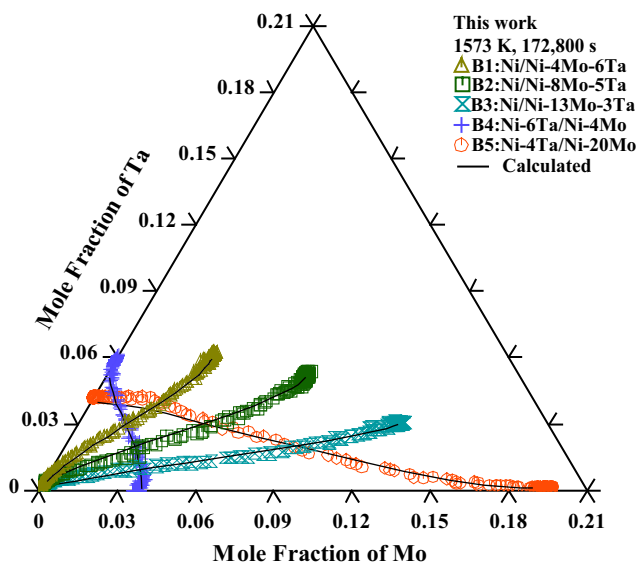

Fig. 6 Comparison between the experimental and DICTRA-simulated diffusion paths for various ternary Ni-Mo-Ta diffusion couples annealed at 1573 for 172,800 s

generally faster than that of Mo. The interdiffusion coefficients obtained require verification by the following constraints,[20]

$$\tilde{D}_{\text{TaTa}}^{\text{Ni}} + \tilde{D}_{\text{MoMo}}^{\text{Ni}} > 0 \qquad (\text{Eq } 12)$$

$$\tilde{D}_{\text{TaTa}}^{\text{Ni}} \cdot \tilde{D}_{\text{MoMo}}^{\text{Ni}} - \tilde{D}_{\text{MoTa}}^{\text{Ni}} \cdot \tilde{D}_{\text{TaMo}}^{\text{Ni}} \geq 0 \qquad (\text{Eq } 13)$$

$$\left(\tilde{D}_{\text{TaTa}}^{\text{Ni}} - \tilde{D}_{\text{MoMo}}^{\text{Ni}}\right)^2 + 4\tilde{D}_{\text{TaMo}}^{\text{Ni}} \cdot \tilde{D}_{\text{MoTa}}^{\text{Ni}} \geq 0 \qquad (\text{Eq } 14)$$

Comprehensive calculation implied that the obtained interdiffusion coefficients satisfy these constraint which are illustrated in Eq 12 to 14. Therefore, the presently obtained interdiffusivities are considered to be reasonable.

4.2 Assessment of Atomic Mobility

Since the assessment of diffusivities is based on thermodynamic description, obtaining more accurate atomic mobilities must depend on reasonable thermodynamic parameters. The thermodynamic assessment of the Ni-Mo-Ta ternary system used in these work is taken from the works of Cui et al.[21] The calculated isothermal section of the Ni-Mo-Ta system at 1473 and 1573 K is shown in Fig. 1(a) and (b), respectively. The alloy compositions of the diffusion couples in the Ni-rich area prepared in the present work at 1473 and 1573 K are shown by schematic diagram in Fig. 1(c) and (d), respectively. The atomic mobilities for the self-diffusion of Ni are taken from Neumann and Tölle[22], and that of Mo and Ta are taken from Liu et al.[9] and Campbell et al.[8], respectively. The atomic mobility parameters of Ni-Mo and Ni-Ta system can be directly acquired from Liu et al.[9] and Campbell et al.[8] Because of the fcc phase of Mo-Ta system is non-equilibrium steady states under common condition, its atomic mobilities is unavailable. For simplification, the impurity diffusion coefficient of Mo in the hypothetical fcc-Ta is assumed to be equivalent to the self-diffusion coefficient of fcc-Ta, and the impurity diffusion coefficient of Ta in the hypothetical fcc-Mo is set to be equal to the self-diffusivity of Mo in the fcc-Mo in the present work. Thus, based on the existing binary atomic mobilities in Table 3 and the experimental interdiffusion coefficients in Table 2, the atomic mobilities of fcc ternary Ni-Mo-Ta alloys were assessed in the PARROT module of the DICTRA software. All of the atomic mobility parameters for Ni-Mo-Ta alloys are listed in Table 3.

Figure 2 illustrates the comparison between the presently calculated main diffusion coefficients and the experimental values, as can be seen, there is a good match between the calculated interdiffusivities and the experimental ones. The calculated logarithmic values of main interdiffusion coefficients are equal to the experimental ones along the diagonal line. The dashed lines with a factor of 2 or 0.5 from the diagonal line are shown as well. Such a factor is a generally accepted experimental error for measurement of diffusivities. The good agreement between the

440

J. Phase Equilib. Diffus. (2019) 40:432–441

calculated results and the experimental ones can been seen from Fig. 2.

4.3 Validation of the Present Atomic Mobility

Verification of the assessed atomic mobility parameters includes not only the comparison with the experimental diffusion coefficients, but also the comparison between the DICTRA-simulated and the observed diffusion behaviors, such as the concentration profiles and the diffusion paths. Figure 3 and 4 present the DICTRA-simulated concentration profiles of the diffusion couples annealed at 1473 K for 259,200 s and that of the diffusion couples annealed at 1573 K for 172,800 s, respectively, together with the corresponding experimental values. The calculated results for different Ni-rich ternary diffusion couples agree well with most of the corresponding experimental values. Figure 5 and 6 present the calculated diffusion paths for various ternary Ni-Mo-Ta diffusion couples annealed at 1473 and 1573 K for 259,200 and 172,800 s, respectively, compared with the corresponding experimental data. As shown in this figure, the diffusion paths almost cover the whole region of the fcc phase in Ni-Mo-Ta alloys. The calculated results and the experimental data have a good agreement, which also proves the validity of the mobility parameters.

5 Conclusions

The composition-dependent ternary interdiffusion coefficients of the fcc Ni-rich Ni-Mo-Ta ternary system at 1473 and 1573 K were determined by means of EPMA technique coupled with the Whittle–Green method in the present work. The reliability of the experimental interdiffusivities is validated via thermodynamic constraints. The uncertainties associated with the measured interdiffusivities were evaluated considering error propagation, meanwhile, by comprehensive comparison between calculated and the experimental results, good agreements were obtained. The diffusion phenomena such as concentration-distance profiles and diffusion paths can be reasonably described. Results show that the values of $\tilde{D}_{TaTa}^{Ni}$ are generally larger than $\tilde{D}_{MoMo}^{Ni}$.

References

1. F. Sun, Y.F. Gu, J.B. Yan, Z.H. Zhong, and M. Yuyama, Phenomenological and Microstructural Analysis of Intermediate Temperatures Creep in a Ni-Fe-Based Alloy for Advanced Ultra-Supercritical Fossil Power Plants, *Acta Mater.*, 2016, **102**, p 70-78
2. C.E. Campbell, Assessment of the Diffusion Mobilites in the γ' and B2 Phases in the Ni-Al-Cr System, *Acta Mater.*, 2008, **56**(16), p 4277-4290
3. L. Rougier, A. Jacot, C.A. Gandin, and P.D. Napoli, Numerical Simulation of Precipitation in Multicomponent Ni-Base Alloys, *Acta Mater.*, 2013, **61**(17), p 6396-6405
4. S. Hata, T. Mitate, N. Kuwano, S. Matsumura, D. Shindo, and K. Oki, Short Range Order Structures in fcc-Based Ni-Mo Studied by High Resolution Transmission Electron Microscopy with Image Processing, *Mat. Sci. Eng. A-Struct.*, 2001, **312**(1), p 160-167
5. T. Yu, Q. Deng, D. Gang, and J. Yang, Effects of Ta on Microstructure and Microhardness of Ni Based Laser Clad Coating, *Appl. Surf. Sci.*, 2011, **257**(11), p 5098-5103
6. P.J. Spencer, A Brief History of CALPHAD, *Calphad*, 2008, **32**(1), p 1-8
7. A. Borgenstam, L. Höglund, J. Ågren, and A. Engström, DICTRA, a Tool for Simulation of Diffusional Transformations in Alloys, *J. Phase Equilib.*, 2000, **21**(3), p 269
8. C.E. Campbell, W.J. Boettinger, and U.R. Kattner, Development of a Diffusion Mobility Database for Ni-Base Superalloys, *Acta Mater.*, 2002, **50**(4), p 775-792
9. X.J. Liu, H.H. Hu, J.J. Han, Y. Lu, and C.P. Wang, Assessment of the Diffusional Mobilities in fcc Ni-Nb and fcc Ni-Mo Alloys, *Calphad*, 2012, **38**(38), p 140-145
10. J. Kirkaldy, Diffusion in Multicomponent Metallic Systems, *Can. J. Phys.*, 2011, **35**(4), p 435-440
11. D. Whittle and A. Green, The Measurement of Diffusion Coefficients in Ternary Systems, *Scr. Metall.*, 1974, **8**(7), p 883-884
12. J. Ågren, Numerical Treatment of Diffusional Reactions in Multicomponent Alloys, *J. Phys. Chem. Solids*, 1982, **43**(4), p 385-391
13. J. Ågren, Diffusion in Phases with Several Components and Sublattices, *J. Phys. Chem. Solids*, 1982, **43**(5), p 421-430
14. J.O. Andersson and J. Ågren, Models for Numerical Treatment of Multicomponent Diffusion in Simple Phases, *J. Appl. Phys.*, 1992, **72**(4), p 1350-1355
15. J.O. Andersson, L. Höglund, B. Jönsson, and J. Ågren, Computer Simulation of Multicomponent Diffusional Transformations in Steel, *Fundam. Appl. Ternary Diffus.*, 1990, **14**, p 153-163
16. B. Jönsson, Ferromagetic Ordering and Diffusion of Carbon and Nitrogen in bcc Cr-Fe-Ni Alloys, *Z. Metallkd.*, 1994, **85**, p 498-501
17. O. Redlich and A. Kister, Algebraic Representation of Thermodynamic Properties and Classification of Solution, *Ind. Eng. Chem.*, 1948, **40**, p 345-348
18. M. Hillert, Empirical Methods of Predicting and Representing Thermodynamic Properties of Ternary Solution Phases, *Calphad*, 1980, **4**(1), p 1-12
19. J.O. Andersson and J. Ågren, Models for Numerical Treatment of Multicomponent Diffusion in Simple Phases, *J. Appl. Phys.*, 1992, **72**(4), p 1350-1355
20. J.S. Kirkaldy, D. Weichert, and Z.U. Haq, Diffusion in Multicomponent Metallic Systems VI. Some Thermodynamic Properties of the D Matrix and the Corresponding Solutions of the Diffusion Equations, *Can. J. Phys.*, 2011, **41**(12), p 2166-2173

21. Y. Cui, Z. Jin, and X. Lu, Experimental Study and Thermody-namic Assessment of the Ni-Mo-Ta Ternary System, *Metall. Mater. Trans. A*, 1999, **30**(11), p 2735-2744

22. G. Neumann and V. Tölle, Monovacancy and Divacancy Con-tributions to Self-Diffusion in Face-Centred Cubic Metals Reanalysis for Copper, Silver, Gold, Nickel and Platinum, *Philos. Mag.*, 1986, **54**(54), p 619-629

Publisher's Note Springer Nature remains neutral with regard to jurisdictional claims in published maps and institutional affiliations.